

# A Genuinely Multi-Dimensional Relaxed Upwind Scheme for Nonlinear Hyperbolic Problems

K. R. ARUN

Department of Mathematics, Indian Institute of Science, Bangalore-560012, India  
E-mail address: arunkr@math.iisc.ernet.in

## Abstract.

In this paper we present the results of a genuinely multi-dimensional relaxed upwind scheme for an arbitrary system of conservation laws in two space dimensions. A new discrete velocity Boltzmann equation is proposed, which is an improvement over the previously introduced models in terms of the isotropic coverage of the multi-dimensional domain by the foot of the characteristic. A finite volume method has been developed in which the fluxes at the cell interfaces are evaluated in a genuinely multi-dimensional way, in contrast to the traditional dimension by dimension treatment. Second order accuracy of the scheme is achieved by using standard MUSCL type reconstructions and TVD Runge-Kutta time discretizations. The results of several numerical experiments on the compressible Euler equations are presented which confirm the robustness and correct multi-dimensional behaviour of the new scheme.

**Key words:** Genuinely multi-dimensional schemes, relaxation systems, isotropy, hyperbolic conservation laws, discrete velocity Boltzmann equation.

## 1. INTRODUCTION

Finite volume methods have been popular for the numerical solution of hyperbolic conservation laws in the last three decades. The finite volume methods have reached a state of maturity for one-dimensional simulations. This development is mainly due to the intense focus of research devoted to the development of upwind methods from 1970s. For multi-dimensional cases, however, the traditional finite volume methods are typically based on a dimension-by-dimension treatment using one-dimensional approximate Riemann solvers. As a result of this inherently one-dimensional treatment, the discontinuities which are oblique to the coordinate directions are not resolved accurately. Developing genuinely multi-dimensional algorithms has been a topic of intense research in the last decade and a half. The reader is referred to [6,17,19] for some multi-dimensional schemes.

Kinetic (or Boltzmann) schemes and relaxation schemes give interesting alternatives to the classical Riemann solver based schemes. Reviews of these methods are available in [7,9,14]. Of these methods, relaxation schemes are the latest and are probably the simplest of all the upwind methods, as they are based on linear convection equations with simple algebraic moment relations leading to conservation laws. A relaxation system converts a nonlinear convection equation into linear convection equations with stiff nonlinear source terms containing a relaxation parameter  $\epsilon$ . Relaxation systems have a strong connection with classical Boltzmann equation of kinetic theory. The diagonal form of a relaxation system for a conservation law can be viewed as a discrete velocity Boltzmann equation, see [1]. The so called discrete kinetic schemes are numerical methods based on the discrete velocity Boltzmann equation, see [1,3,16].

There has been numerous approaches in the literature to derive numerical approximations of nonlinear conservation laws using relaxation systems. The numerical methods developed using a relaxation system can be classified into two categories: relaxing schemes and relaxed schemes [11]. A relaxing scheme can be obtained by discretizing a relaxation system and hence they contain the parameter  $\epsilon$  explicitly. The presence of  $\epsilon$  introduces stiffness in the problem and it is a very challenging task to obtain a high order numerical approximation, see [12,15] for more details. On the

contrary, a relaxed scheme is the limit of a relaxing scheme as the relaxation parameter  $\epsilon$  goes to 0. Hence, a relaxed scheme is independent of  $\epsilon$  and is a stable discretization of the given conservation law,[11]. We refer the reader to [18] for some high resolution relaxed schemes.

The goal of this paper is to develop a genuinely multi-dimensional relaxed scheme for two-dimensional hyperbolic systems using a discrete velocity Boltzmann equation. In [2] the authors have introduced a new discrete Boltzmann equation in which the foot of the characteristic traverses all quadrants in an isotropic way. Using the isotropy of this relaxation system, we design a high resolution relaxed upwind scheme in a finite volume framework. The scheme achieves second order accuracy by using MUSCL type reconstructions. Like upwind schemes, the reconstructed piecewise polynomials used by our scheme also make use of nonlinear limiters which guarantee the overall non-oscillatory nature of the approximate solution. One remarkable feature of the relaxed schemes is that they avoid the solution of complex Riemann problems or characteristic decompositions which are essential for high resolution upwind schemes. This advantage is particularly important in multidimensional problems, where there is no exact Riemann solvers.

The organisation of this paper is as follows. In section 2 we introduce relaxation systems for a system of conservation laws in two space dimensions. The numerical discretization of the relaxation system and the derivation of a semi-discrete relaxed scheme is presented in section 3. The results of extensive numerical experiments are reported in section 4. Finally, we close this paper with some concluding remarks in section 5.

## 2. RELAXATION SYSTEMS FOR HYPERBOLIC CONSERVATION LAWS

In this section we introduce relaxation systems for a system of conservation laws in two space dimensions. It is straight forward to extend the results to arbitrary space dimensions. Consider the Cauchy problem

$$u_t + g_1(u)_x + g_2(u)_y = 0, \quad (2.1)$$

$$u(x, y, 0) = u_0(x, y), \quad (2.2)$$

where  $u \in \mathcal{U} \subset \mathbb{R}^m$  (a convex open set) is unknown and  $g_j$  maps  $\mathcal{U}$  to  $\mathbb{R}^m$ . As in [1] we assume that the system (2.1) is endowed with a family of strictly convex entropies. The discrete BGK models constructed in [1] are of the form

$$f_{kt} + a(k) \cdot \nabla_x f_k = \frac{1}{\epsilon} (F_k(u) - f_k), \quad (2.3)$$

for  $k \in \{1, 2, \dots, N\}$ . Here  $f_k = f_k(x, y, t) \in \mathbb{R}^m$  is unknown,  $a(k) \in \mathbb{R}^2$  is a constant vector with components  $a_j(k)$  ( $j=1, 2$ ),  $a(k) \cdot \nabla_x = a_1(k)\partial_x + a_2(k)\partial_y$ ,  $u = \sum_{k=1}^N f_k$  and the so called Maxwellians  $F_k: \mathcal{U} \rightarrow \mathbb{R}^m$  satisfy the consistency relations

$$\sum_{k=1}^N F_k(u) = u, \quad \sum_{k=1}^N a_j(k) F_k(u) = g_j(u) \quad \forall u \in \mathcal{U}. \quad (2.4)$$

Following Bouchut [4], we choose  $F_k(u)$  to be linear combinations of  $u$  and  $g_j(u)$ , i.e.,

$$F_k(u) = \alpha_{k0}u + \alpha_{k1}g_1(u) + \alpha_{k2}g_2(u), \quad (2.5)$$

where the coefficients  $\alpha_{kj}$  are to be chosen so that the consistency conditions (2.4) are satisfied. As in [2], we take  $N = 4$  and choose discrete velocities  $a(k)$  to be<sup>1</sup>

<sup>1</sup>Henceforth, we use only the choice (2.6) for the discrete velocities.

$$\begin{aligned} a(1) &= (-\lambda, -\lambda), & a(2) &= (\lambda, -\lambda), \\ a(3) &= (\lambda, \lambda), & a(4) &= (-\lambda, \lambda). \end{aligned} \tag{2.6}$$

A simple calculation yields

$$\begin{aligned} F_1(u) &= \frac{u}{4} - \frac{g_1(u)}{4\lambda} - \frac{g_2(u)}{4\lambda}, & F_2(u) &= \frac{u}{4} + \frac{g_1(u)}{4\lambda} - \frac{g_2(u)}{4\lambda}, \\ F_3(u) &= \frac{u}{4} + \frac{g_1(u)}{4\lambda} + \frac{g_2(u)}{4\lambda}, & F_4(u) &= \frac{u}{4} - \frac{g_1(u)}{4\lambda} + \frac{g_2(u)}{4\lambda}. \end{aligned} \tag{2.7}$$

We now introduce two new variables  $v_1$  and  $v_2$  via

$$v_j = \sum_{k=1}^4 a_j(k) f_k, \quad j = 1, 2 \tag{2.8}$$

and let

$$f_k = \beta_{k0}u + \beta_{k1}v_1 + \beta_{k2}v_2. \tag{2.9}$$

Since  $\sum_{k=1}^4 f_k = u$  and using (2.8) we can immediately arrive at

$$\begin{aligned} f_1 &= \frac{u}{4} - \frac{v_1}{4\lambda} - \frac{v_2}{4\lambda}, & f_2 &= \frac{u}{4} + \frac{v_1}{4\lambda} - \frac{v_2}{4\lambda}, \\ f_3 &= \frac{u}{4} + \frac{v_1}{4\lambda} + \frac{v_2}{4\lambda}, & f_4 &= \frac{u}{4} - \frac{v_1}{4\lambda} + \frac{v_2}{4\lambda}. \end{aligned} \tag{2.10}$$

Multiplying (2.3) successively by 1,  $a_1(k)$ ,  $a_2(k)$  and taking summation over  $k$  yields a Jin-Xin [11] type relaxation model

$$u_t + v_{1x} + v_{2y} = 0, \tag{2.11}$$

$$v_{1t} + \lambda^2 u_x = \frac{1}{\epsilon} (g_1(u) - v_1), \tag{2.12}$$

$$v_{2t} + \lambda^2 u_y = \frac{1}{\epsilon} (g_2(u) - v_2). \tag{2.13}$$

Note that in the limit  $\epsilon \rightarrow 0$ , (2.12)-(2.13) formally gives

$$v_1 = g_1(u), \quad v_2 = g_2(u) \tag{2.14}$$

and from (2.11) the original conservation law (2.1) can be recovered.

The parameter  $\lambda$  appearing in (2.12)-(2.13) has to be chosen according to some stability condition. There are several approaches in the literature to study the stability of relaxation systems. We refer the reader to [4,5] for more details. In our calculations we have used the entropy extension condition of Bouchut [4], i.e,

$$\sigma (F'_k(u)) \subset [0, \infty[, \quad \forall k, \tag{2.15}$$

where  $\sigma (F'_k(u))$  denotes the spectrum of  $F'_k(u)$ .

It is to be remarked that the particular choice (2.6) of discrete velocities  $a(k)$  admits the following nice feature, which we call isotropy. The characteristic curves of (2.3) through any point  $P(x, y, t + \Delta t)$  fall

evenly in all the four quadrants around the point  $Q(x, y, t)$ , see figure 1.

Note that isotropy is a special property of our relaxation system. This feature enables us to design a genuinely multi-dimensional finite volume scheme for (2.3).

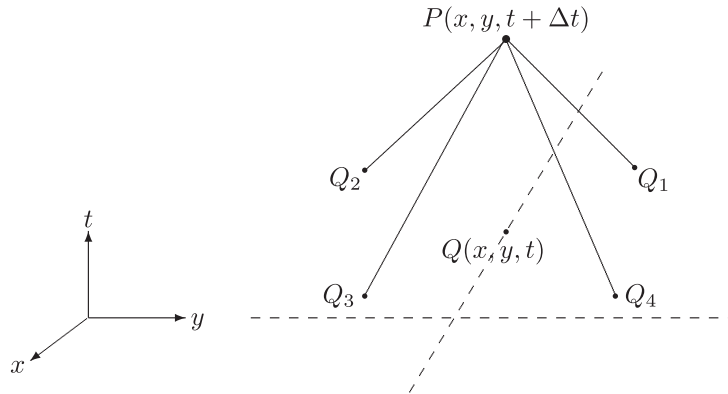


Figure 1. Feet of the characteristics covering the multi-dimensional domain in an isotropic way.

### 3. RELAXED UPWIND SCHEMES

A relaxation system provides a novel method for the numerical approximation of nonlinear systems of conservation laws. The first numerical experiments using a relaxation system has been reported by Jin and Xin [11]. These authors classify their schemes as relaxing schemes and relaxed schemes. A relaxing scheme is discretization of a relaxation system and hence they contain the parameter  $\epsilon$  explicitly. For instance a semi-discrete discretization of relaxation system of the type (2.11)-(2.13) give rise to a stiff system of ordinary differential equations. It is well known that deriving a higher order approximation of a stiff system is a very challenging task. On the other hand, a relaxed scheme is the limit of a relaxing scheme as  $\epsilon \rightarrow 0$  and they give a stable discretization of the original conservation law. The goal of the present work is to develop a genuinely multi-dimensional relaxed scheme using the isotropy of the relaxation system (2.3) introduced in section 2.

Let  $\Omega$  be our two-dimensional computational domain. We introduce a rectangular grid which for simplicity is assumed to be uniform with mesh size  $h = \Delta x = \Delta y$  in both the directions. Let us denote by  $\Omega_{i,j}$  the cell centred around the point  $(x_i, y_j)$ , i.e.,  $\Omega_{i,j} = [x_i - h/2, x_i + h/2] \times [y_j - h/2, y_j + h/2]$ . Let  $\Delta t$  be the time step and denote  $w_{i,j}^n$  the point value of a function  $w$  at the  $(i,j)$ -th mesh point at time  $t^n = n\Delta t$ . Finally let  $\bar{w}_{i,j}(t)$  be the cell average of the function  $w$  taken over  $\Omega_{i,j}$ , i.e.,

$$\bar{w}_{i,j}(t) = \frac{1}{h^2} \int_{\Omega_{i,j}} w(x, y, t) dx dy. \tag{3.1}$$

Given the cell averages  $\bar{w}_{i,j}^n$  at time level  $t^n$ , a piecewise linear reconstruction is done resulting in

$$w^n(x, y) = \sum_{i,j} P_{i,j}(x, y; w) \mathbf{1}_{i,j}(x, y). \tag{3.2}$$

Here  $P_{i,j}(x, y; w)$  is a vector valued linear polynomial given by

$$P_{i,j}(x, y; w) = \bar{w}_{i,j}^n + w_{i,j}^x \left( \frac{x - x_i}{\Delta x} \right) + w_{i,j}^y \left( \frac{y - y_j}{\Delta y} \right) \tag{3.3}$$

and  $\mathbf{1}_{i,j}$  is the characteristic function of the cell  $\Omega_{i,j}$ . The quantities  $w_{i,j}^x, w_{i,j}^y$  are respectively the discrete

slopes in  $x$ - and  $y$ -directions. A possible computation of these slopes which results in an overall non-oscillatory scheme is given by [10]

$$w_{i,j}^x = MM \left( \theta \Delta \bar{w}_{i+\frac{1}{2},j}, \frac{1}{2} \left( \Delta \bar{w}_{i-\frac{1}{2},j} + \Delta \bar{w}_{i+\frac{1}{2},j} \right), \theta \Delta \bar{w}_{i-\frac{1}{2},j} \right), \quad (3.4)$$

$$w_{i,j}^y = MM \left( \theta \Delta \bar{w}_{i,j+\frac{1}{2}}, \frac{1}{2} \left( \Delta \bar{w}_{i,j-\frac{1}{2}} + \Delta \bar{w}_{i,j+\frac{1}{2}} \right), \theta \Delta \bar{w}_{i,j-\frac{1}{2}} \right). \quad (3.5)$$

Here  $\Delta$  is a finite difference operator defined by  $\Delta \bar{w}_{i+\frac{1}{2},j} := \bar{w}_{i+1,j} - \bar{w}_{i,j}$ , the parameter  $\theta$  takes values in the interval  $[1,2]$  and  $MM$  denotes the general minmod function defined by

$$MM \{x_1, x_2, \dots\} := \begin{cases} \min_p \{x_p\}, & \text{if } x_p > 0 \ \forall p, \\ \max_p \{x_p\}, & \text{if } x_p < 0 \ \forall p, \\ 0, & \text{otherwise.} \end{cases} \quad (3.6)$$

We solve the discrete kinetic equation (2.3) by a splitting method

$$f_{k,t} + a(k) \cdot \nabla_x f_k = 0, \quad (\text{convection step}) \quad (3.7)$$

$$\frac{df_k}{dt} = \frac{1}{\epsilon} (F_k(u) - f_k). \quad (\text{collision step}) \quad (3.8)$$

Since  $\sum_{k=1}^4 f_k = \sum_{k=1}^4 F_k(u) = u$ , summing over  $k$  on both sides of (3.8) to obtain

$$\frac{du}{dt} = 0. \quad (3.9)$$

Thus,  $u \equiv u^*$ , where  $u^*$  is an initial value for (3.9). Hence we conclude that the macroscopic conserved variable  $u$  remains constant during the collision step in the splitting scheme (3.7)-(3.8). Multiplying (3.8) by  $a_j(k)$  and summing over  $k$  yields

$$\frac{dv_j}{dt} = \frac{1}{\epsilon} (g_j(u) - v_j). \quad (3.10)$$

Since  $u \equiv u^*$  the equation (3.10) can be solved exactly. It is easy to verify that this solution in the limit  $\epsilon \rightarrow 0$  gives

$$v_j = g_j(u^*). \quad (3.11)$$

Thus,  $v_j$  relaxes to its equilibrium value  $g_j(u^*)$  instantaneously after every convection step. This is analogous to the philosophy of kinetic schemes. Hence we need to solve only the linear convection equations in (3.7) apart from enforcing the condition  $v_j(\cdot, t^n) = g_j(u(\cdot, t^n))$ ,  $j=1, 2$ . Also note that the relaxation parameter  $\epsilon$  has disappeared and accordingly all the stiffness related problems are removed.

Integrating (3.7) over the control volume  $\Omega_{ij}$  yields a semi-discrete scheme for the evolution of the cell averages  $\bar{f}_{ki,j}$

$$\frac{d\bar{f}_{ki,j}}{dt} = -\frac{\mathcal{A}_{k,i+\frac{1}{2},j} - \mathcal{A}_{k,i-\frac{1}{2},j}}{h} - \frac{\mathcal{B}_{k,i,j+\frac{1}{2}} - \mathcal{B}_{k,i,j-\frac{1}{2}}}{h}, \quad (3.12)$$

where

$$\mathcal{A}_{k_{i+\frac{1}{2},j}} = \frac{1}{h} \int_{y_{j-\frac{1}{2}}}^{y_{j+\frac{1}{2}}} a_1(k) f_k(x_{i+\frac{1}{2}}, y, t) dy \quad (3.13)$$

and an analogous expression exists for  $\mathcal{B}_{k_{i,j+\frac{1}{2}}}$ . We now take summation over  $k$  on (3.12) to get a semi-discrete scheme for the cell averages  $\bar{u}_{i,j}$  of the macroscopic conserved variable  $u$

$$\frac{d\bar{u}_{i,j}}{dt} = -\frac{\mathcal{F}_{i+\frac{1}{2},j} - \mathcal{F}_{i-\frac{1}{2},j}}{h} - \frac{\mathcal{G}_{i,j+\frac{1}{2}} - \mathcal{G}_{i,j-\frac{1}{2}}}{h}, \quad (3.14)$$

where

$$\begin{aligned} \mathcal{F}_{i+\frac{1}{2},j} &= \sum_{k=1}^4 \mathcal{A}_{k_{i+\frac{1}{2},j}} \\ &= \frac{1}{h} \int_{y_{j-\frac{1}{2}}}^{y_{j+\frac{1}{2}}} \sum_{k=1}^4 a_1(k) f_k(x_{i+\frac{1}{2}}, y, t) dy, \\ &= \frac{1}{h} \int_{y_{j-\frac{1}{2}}}^{y_{j+\frac{1}{2}}} v_1(x_{i+\frac{1}{2}}, y, t) dy. \end{aligned} \quad (3.15)$$

A similar expression can be derived for  $\mathcal{G}_{i,j+\frac{1}{2}}$ . Therefore it can be concluded that if we use a p-th order high resolution fluxin (3.14) and a p-th order SSP Runge-Kutta for time integration then we can achieve an overall p-th order accurate scheme for the original conservation law (2.1).

We now turn to develop a genuinely multi-dimensional procedure for evaluating numerical fluxes  $\mathcal{F}$  and  $\mathcal{G}$ . As a first step, we approximate the flux integral in (3.15) using Simpson's quadrature to get

$$\begin{aligned} \mathcal{F}_{i+\frac{1}{2},j} &= \frac{1}{h} \int_{y_{j-\frac{1}{2}}}^{y_{j+\frac{1}{2}}} v_1(x_{i+\frac{1}{2}}, y, t) dy, \\ &= \frac{1}{6} (v_1^{NE} + 4v_1^E + v_1^{SE}), \end{aligned} \quad (3.16)$$

where we have denoted

$$v_1^Q = v_1(x_Q, y_Q, t), \quad Q \in \{NE, E, SE\}. \quad (3.17)$$

Note that using (2.8) we can obtain

$$v_1^{NE} = -\lambda f_1^{NE} + \lambda f_2^{NE} + \lambda f_3^{NE} - \lambda f_4^{NE}. \quad (3.18)$$

Therefore, we need to reconstruct the point values of  $f_k, k \in \{1,2,3,4\}$  at the quadrature node NE. This is can be achieved by exploiting the upwind information based on the advection velocities of  $f_k$  to yield

$$f_1^{NE} = P_{i+1,j+1}(x_{NE}, y_{NE}; f_1). \quad (3.19)$$

Analogously we can get

$$f_2^{NE} = P_{i,j+1}(x_{NE}, y_{NE}; f_2), \quad (3.20)$$

$$f_3^{NE} = P_{i,j}(x_{NE}, y_{NE}; f_3), \tag{3.21}$$

$$f_4^{NE} = P_{i+1,j}(x_{NE}, y_{NE}; f_4). \tag{3.22}$$

In a similar way we can derive the interpolated values of  $f_k$  at the quadrature nodes E and SE also. It is to be remarked that this way the use of Simpson rule in the approximation of the flux integral (3.16) takes into consideration the cross wind direction also. Finally the isotropy of our relaxation model helps to incorporate the contribution from the cells  $\Omega_{i+k,j+l,k} \in \{0,1\}, l \in \{-1,0,1\}$  in the evaluation of the flux  $\mathcal{F}_{i+\frac{1}{2},j}$  through a right vertical edge. A floor plan of the quadrature nodes used in this genuinely multi-dimensional flux evaluation procedure is given in figure 2. The expression for the flux  $\mathcal{G}_{i,j+\frac{1}{2}}$  through a top horizontal edge can be derived along the same lines.

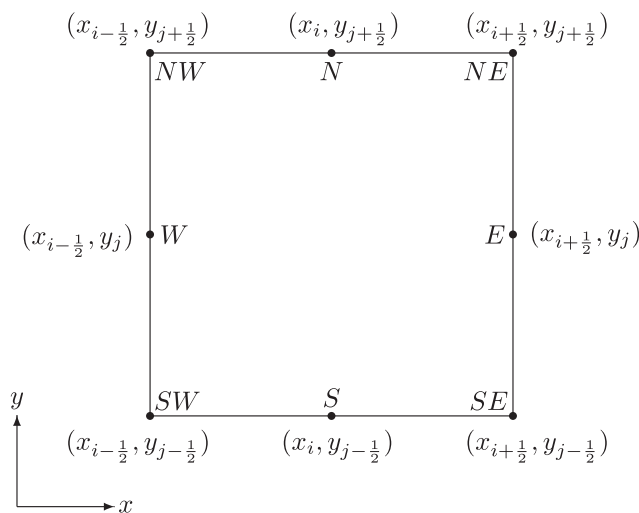


Figure 2. Quadrature nodes used in the multi-dimensional flux evaluation.

To improve the temporal accuracy and to gain second order accuracy in time we use a TVD Runge-Kutta scheme to numerically integrate the system of ODEs (3.14). Denoting the right hand side of (3.14) by  $\mathcal{L}(u)$ , the second order Runge-Kutta scheme update  $u$  through the following two stages

$$u^{(1)} = u^n + \Delta t \mathcal{L}(u^n), \tag{3.23}$$

$$u^{n+1} = \frac{1}{2}u^n + \frac{1}{2}u^{(1)} + \frac{1}{2}\Delta t \mathcal{L}(u^{(1)}). \tag{3.24}$$

#### 4. NUMERICAL CASE STUDIES

We will now present the results of some numerical experiments with our scheme on systems of nonlinear conservation laws in two space dimensions. As prototype of a system of conservation laws we consider the Euler equations

$$\begin{pmatrix} \rho \\ \rho u \\ \rho v \\ E \end{pmatrix}_t + \begin{pmatrix} \rho u \\ \rho u^2 + p \\ \rho uv \\ (E + p)u \end{pmatrix}_x + \begin{pmatrix} \rho v \\ \rho uv \\ \rho v^2 + p \\ (E + p)v \end{pmatrix}_y = 0,$$

where the energy density  $E$  is given by  $E = \frac{p}{(\gamma-1)} + \frac{1}{2}\rho(u^2 + v^2)$ ,  $\gamma = 1.4$  being the gas constant.

The expression for the parameter  $\lambda$  given by the stability condition (2.15) can be explicitly obtained as

$$\lambda = \max\{|u| + |v| + \sqrt{2}a\}$$

where  $a = \sqrt{\gamma p/\rho}$  is the sound speed and the maximum is taken over all mesh cells.

*Test case 1: Experimental Order of Convergence.* Despite the simplicity of the algorithm and operator splitting approach, the relaxed upwind scheme gives second order convergence. In what follows we test the order of convergence for a smooth solution. We consider a smooth periodic solution of the two dimensional Euler equations

$$\begin{aligned}\rho(x, y, t) &= 1.0 + 0.2 \sin(\pi(x + y - t(u + v))), \\ u(x, y, t) &= v(x, y, t) = p(x, y, t) = 1.0.\end{aligned}$$

The experimental order of convergence (EOC) can be calculated by systematically refining the mesh and examining the behaviour of the global error. Since the exact solution is known, the order of convergence in a certain norm  $\|\cdot\|$  can be computed in the following way

$$\text{EOC} = \log_2 \left( \frac{\|w_{N/2}^n - w_{ref}^n\|}{\|w_N^n - w_{ref}^n\|} \right),$$

where  $N$  denotes the number of mesh points in both  $x$ - and  $y$ - directions,  $w$  denotes the approximate and  $w_{ref}$  the exact solution. A suitable choice of norm  $\|\cdot\|$  is  $L^2$  or  $L^1$ . The computational domain  $[-1,1] \times [-1,1]$  is consecutively divided into  $20 \times 20, 40 \times 40, \dots, 320 \times 320$  cells. The final time was taken to be  $t=1.0$ . The table 1 shows the experimental order of convergence computed in the  $L^1$  and  $L^2$  norms. We have used density to compute the errors. From the table it is evident that the order of convergence is 2.

**Table 1.  $L^1$  and  $L^2$  errors with experimental order of convergence for a smooth periodic test case.**

$N$	$L^1$ error	EOC	$L^2$ error	EOC
20	0.01801515		0.01993357	
40	0.00332742	2.4367	0.00369252	2.4325
80	0.00071280	2.2228	0.00079185	2.2213
160	0.00016955	2.0717	0.00018834	2.0719
320	0.00004183	2.0192	0.00004647	2.0188

*Test case 2: Cylindrical explosion problem.* This test case is a two-dimensional Sod problem with a circular discontinuity. The computational domain is the square  $[-1,1] \times [-1,1]$  and the initial data read,

$$\begin{aligned}\rho &= 1, & u &= 0, & v &= 0, & p &= 1, & |\mathbf{x}| < 0.4, \\ \rho &= 0.125, & u &= 0, & v &= 0, & p &= 0.1, & \text{else.}\end{aligned}$$

The solution is computed at time  $t=0.2$  on a  $400 \times 400$  mesh with a CFL number 0.95 using the second order accurate method. The solution exhibits a circular shock and a circular contact discontinuity moving away from the centre of the circle and a circular rarefaction wave moving in the opposite

direction. In this problem we have used absorbing boundary conditions by simple second order extrapolation of the variables. The isolines of density,  $x$ -,  $y$ - components of velocity and pressure are given in figure3. It is evident from figure3 that the scheme resolves circular shocks and contacts very accurately, confirming its genuinely multi-dimensional nature.

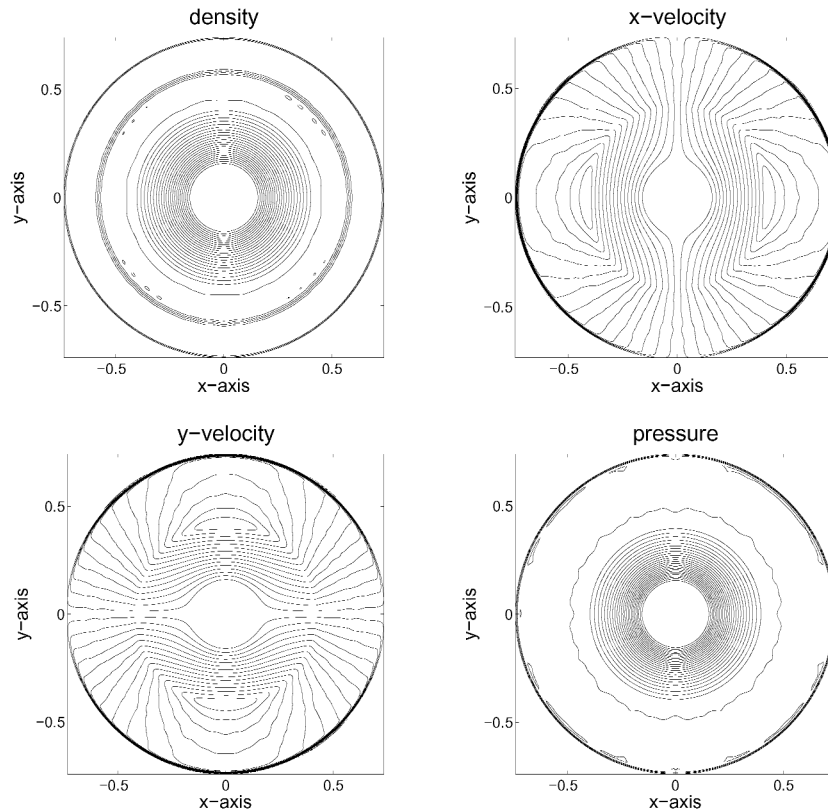


Figure 3. Cylindrical explosion: Isolines of the solution calculated on a  $400 \times 400$  mesh at time  $t = 0.2$ .

*Test case 3: Two-dimensional Riemann problem.* Next test case is a two-dimensional Riemann problem. The computational domain  $[-1,1] \times [-1,1]$  is divided into four quadrants. The initial data consist of single constant states in each of these four quadrants. These constant values are chosen in such a way that each pair of quadrants defines a one-dimensional Riemann problem.

We choose the initial values in such a way that two forward moving shocks and two standing slip lines are produced. The initial data read,

$$(\rho, u, v, p) = \begin{cases} (0.5313, 0, 0, 0, 0, 0.4) & \text{if } x > 0, y > 0, \\ (1, 0, 0, 0, 0.7276, 1, 0) & \text{if } x > 0, y < 0, \\ (1, 0, 0.7276, 0, 0, 1, 0) & \text{if } x < 0, y > 0, \\ (0.8, 0, 0, 0, 0, 1, 0) & \text{if } x < 0, y < 0, \end{cases}$$

The solution is computed at time  $t = 0.52$  with a CFL number 0.95 with both first order and second order methods. The isolines of the density is given in figure 4. It is evident from the figure that the second order method resolves the shocks and slip lines very accurately.

*Test case 4: Explosion in a box problem.* In this example we consider a two-dimensional Riemann

problem with solid boundaries. The setup consists of a square box of side length 2 units with reflecting walls. Initially the density is unity everywhere and the velocities are zero. The pressure is equal to 1000 inside a square of side length 0.5 units at the centre of the box and 10 elsewhere. The computations are done on a  $400 \times 400$  mesh using the second order method. The isolines of density, velocity components and pressure at times  $t = 0.03$  and  $t = 0.1$  are given in figures 5 and 6.

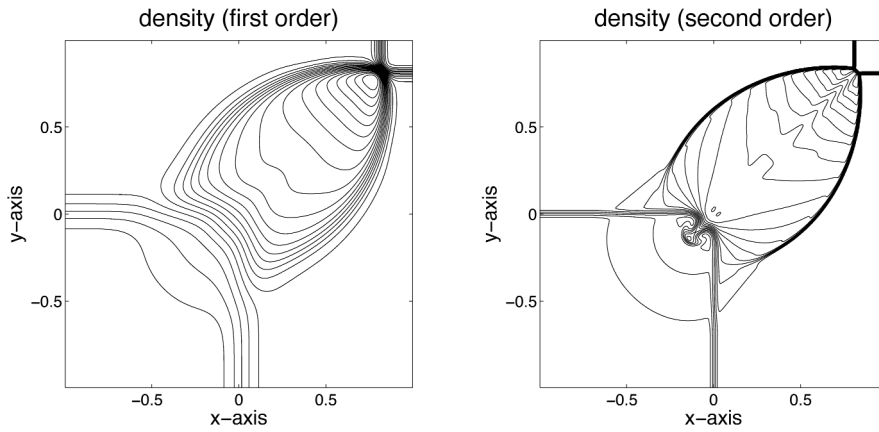


Figure 4. Two dimensional Riemann problem containing two shocks/two slip lines. Isolines of density calculated on a  $400 \times 400$  mesh at time  $t = 0.52$  with first order method (left) and second order method (right).

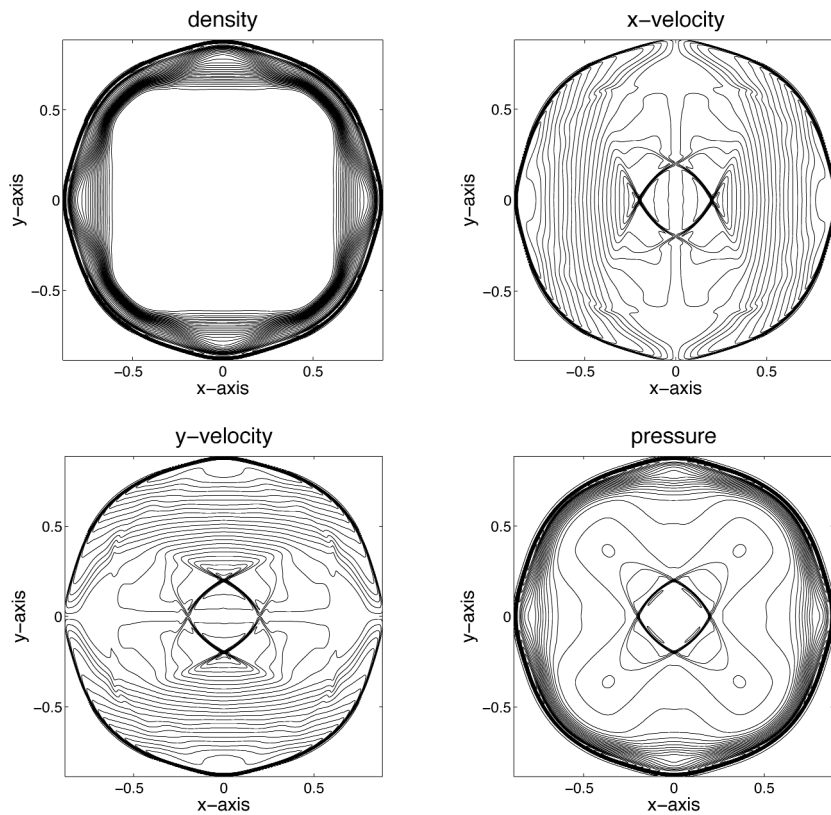


Figure 5. Explosion in a box: Isolines of the solution calculated on a  $400 \times 400$  mesh at time  $t = 0.03$ .

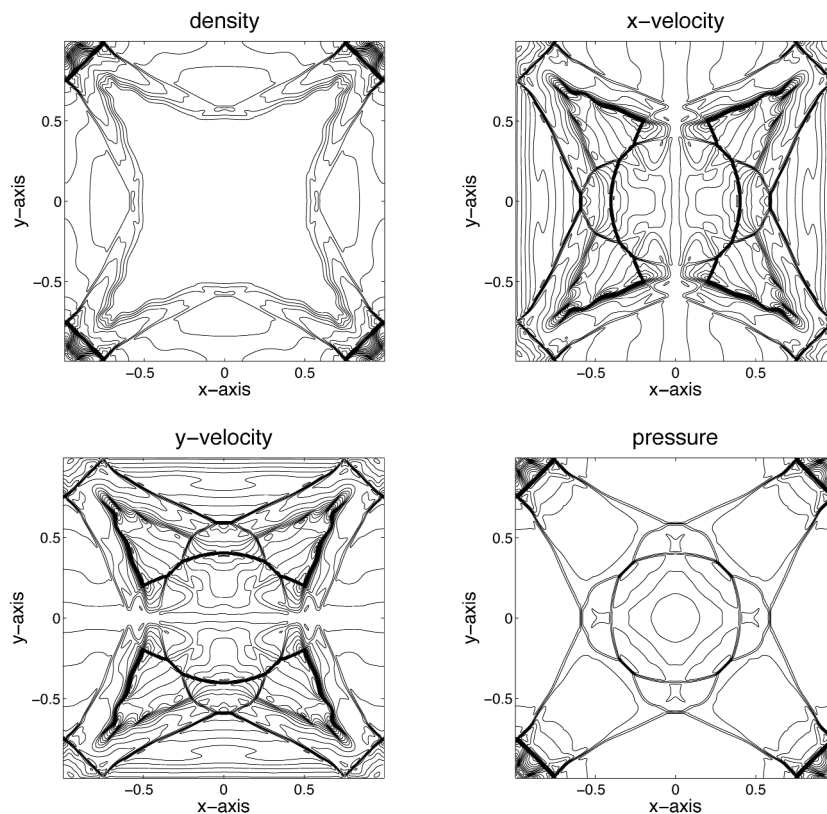


Figure 6. Explosion in a box at time  $t=0.1$ .

*Test case 5: Interaction of two spherically symmetric fields.* This problem was studied by Dreyer et.al [8]. The initial values taken here are slightly different from that of [8]. The computational domain is  $[-1,1] \times [-1,1]$ . The initial data reads:  $\rho(x, y) = 4$ ,  $p(x, y) = 4$  for  $(x + 0.2)^2 + (y + 0.2)^2 \leq 0.6$  and for  $(x - 0.2)^2 + (y - 0.2)^2 \leq 0.6$ . Otherwise  $\rho(x, y) = 1$ ,  $p(x, y) = 1$ . The velocities are zero everywhere. We have used outflow boundary conditions. The results of the second order scheme at time  $t=0.45$  are given in figure 7.

*Test case 6: Shock-bubble interaction problem.* The simulations in this example shows the interaction between a planar shock and various heterogeneities. The motivation for this problem is the 3-D shock bubble interaction studied by Langseth and LeVeque [13]. The problem setup is as follows. A bubble of radius 0.2 lies at rest at  $(0.4, 0.5)$  in the domain  $[0, 1.6] \times [0, 1]$ . The gas is at rest initially and has unit density and pressure. The density inside the bubble is 0.1 while the velocities and pressure has same values as outside. The incoming shock wave starts at  $x = 0.1$  and propagates in the positive  $x$ -direction. Behind the shock the density is 3.81, pressure is 10,  $x$ -velocity is 2.85 and  $y$ -velocity is 0. The schlieren images of the density for different time from  $t = 0.1$  to  $t = 0.4$  is given in figure 8. We have used reflecting boundary conditions on the top and bottom boundaries. The right boundary has outflow boundary conditions whereas the left is inflow boundary.

## 5. CONCLUDING REMARKS

A novel genuinely multi-dimensional relaxed upwind scheme is presented, based on a multi-dimensional relaxation system in which the foot of the characteristics traverses all quadrants in an isotropic way. Second order accuracy of the scheme is achieved by using standard MUSCL type reconstructions and TVD Runge-Kutta time discretizations. The numerical scheme is stable up to a CFL number 1.0. The scheme is tested on some bench-mark problems for Euler equations in two dimensions and the results demonstrate its efficiency in capturing the flow features accurately. The extension of the present scheme to three dimensional problems is straight forward. The relaxed scheme retains all the attractive features of central schemes such as neither Riemann solvers nor characteristic decompositions are needed.

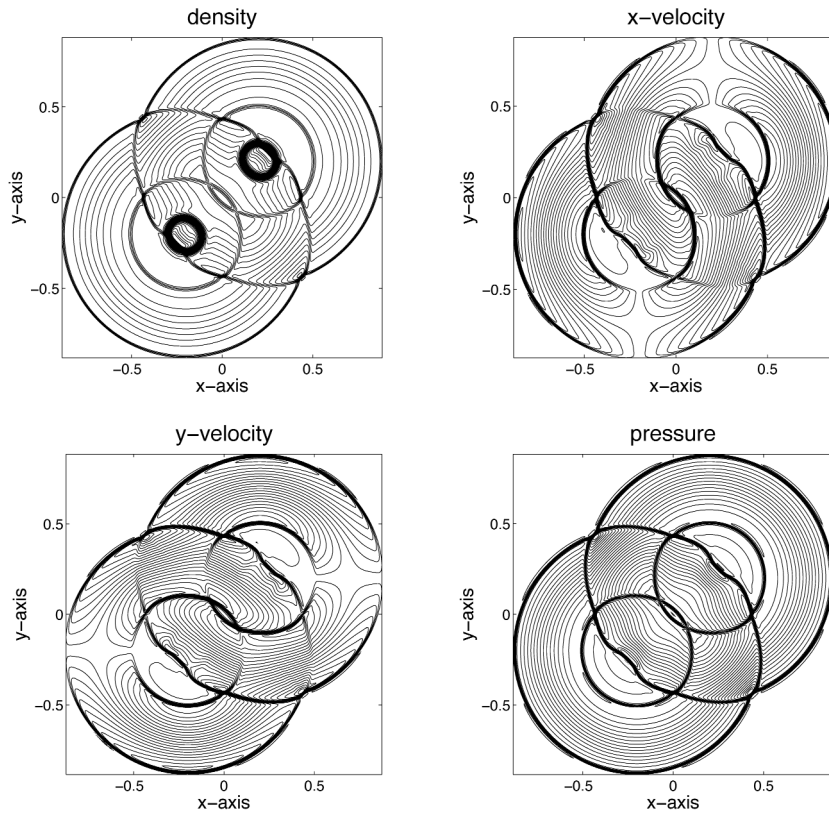


Figure 7. Interaction of two spherically symmetric fields. The isolines of the solution computed on a  $400 \times 400$  mesh at time  $t = 0.45$ .

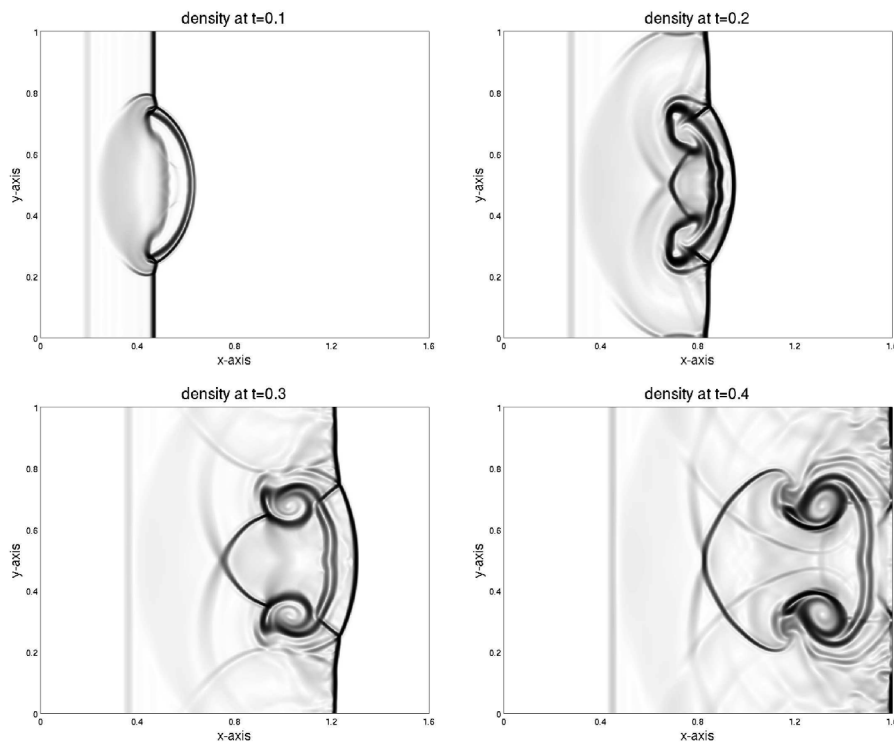


Figure 8. Shock-bubble interaction problem: schlieren images of the density at different times from  $t = 0.1$  to  $t = 0.4$  calculated with second order scheme on a  $640 \times 400$  mesh.

## ACKNOWLEDGEMENT

The author expresses his sincere gratitude to Prof. Phoolan Prasad, Prof. M. Lukáčová-Medvid'ová and Dr. S. V. Raghurama Rao for their constant encouragement and support. He also wish to thank the Council of Scientific & Industrial Research (CSIR) for supporting his research at the Indian Institute of Science (IISc) under the grant-09/079(2084)/2006-EMR-1. The Department of Mathematics at IISc is supported by UGC under SAP.

## REFERENCES

- [1] D. Aregba-Driollet and R. Natalini. Discrete kinetic schemes for multidimensional systems of conservation laws. *SIAM J. Numer. Anal.* 37:1973-2004, 2000.
- [2] K. R. Arun, S. V. Raghurama Rao, M. Lukáčová-Medvid'ová and P. Prasad. A genuinely multi-dimensional relaxation scheme for hyperbolic conservation laws. In *Proceedings of the Seventh Asian CFD conference, Bangalore, 2007*.
- [3] S. Balasubramanyam and S. V. Raghurama Rao. A grid free upwind relaxation scheme for inviscid compressible flows. *Int. J. Numer. Meth. Fl.* 51:159-196, 2006.
- [4] F. Bouchut. Construction of BGK models with a family of kinetic entropies for a given system of conservation laws. *J. Stat. Phys.* 95:113-170, 1999.
- [5] G. Q. Chen, D. Levermore and T. P. Liu. Hyperbolic conservation laws. with stiff relaxation terms and entropy. *Comm. Pure. Appl. Math.* 47:787-830, 1994.
- [6] P. Colella. Multidimensional upwind methods for hyperbolic conservation laws. *J. Comput. Phys.* 87:171-200, 1990.
- [7] S. M. Deshpande. Kinetic flux splitting schemes. In *Computational Fluid Dynamics Review 1995: A State-of-the-Art Reference to the Latest Developments in CFD*, M. M. Hafez and A. K. Oshima (eds). Wiley: Chichester, 1995.
- [8] W. Dreyer, M. Kunik, K. Sabelfeld, N. Simonov and K. Wilmanski. Iterative procedure for multidimensional Euler equations. *Monte Carlo Methods Appl.* 4:253-271, 1998.
- [9] E. Godlewski and P. A. Raviart. *Numerical Approximations of Hyperbolic Systems of Conservation Laws*. Applied Mathematics Series, vol. 118. Springer: Berlin, 1996.
- [10] G. S. Jiang and E. Tadmor. Nonoscillatory central schemes for multidimensional hyperbolic conservation laws. *SIAM J. Sci. Comput.* 19:1892-1917, 1998.
- [11] S. Jin and Z. Xin. The relaxation schemes for systems of conservation laws in arbitrary space dimensions. *Commun. Pure Appl. Math.* 48:235-276, 1995.
- [12] S. Jin. Runge-Kutta Methods for Hyperbolic Conservation Laws with Stiff Relaxation Terms. *J. Comput. Phys.* 122:51-67, 1995.
- [13] J. O. Langseth and R. J. LeVeque. A wave propagation method for three-dimensional hyperbolic conservation laws. *J. Comput. Phys.* 165:126-166, 2000.
- [14] R. Natalini. Recent mathematical results on hyperbolic relaxation problems, Analysis of systems of conservation laws, Pitman Research Notes in Mathematics Series, Longman, Harlow, 1998.
- [15] L. Pareschi and G. Russo. Implicit-Explicit Runge-Kutta methods and applications to hyperbolic systems with relaxation. *J. Sci. Comput.* 25:129-155, 2005.
- [16] S. V. Raghurama Rao and K. Balakrishna. An accurate shock capturing algorithm with a relaxation system for hyperbolic conservation laws. *AIAA Paper No. AIAA-2003-4115*.
- [17] P. Roe. Discrete models for the numerical analysis of time-dependent multidimensional gas dynamics. *J. Comput. Phys.* 63:458-476, 1986.
- [18] H. J. Schroll. Relaxed high resolution schemes for hyperbolic conservation laws. *J. Sci. Comp.* 21:251-279, 2004.
- [19] B. Van Leer. Progress in multi-dimensional upwind differencing. *ICASE Report No. 92-43*, 1992.

